

Molecular effects in the ionization of N₂, O₂ and F₂ by intense laser fields

Daniel Dundas* and Jan M Rost

Max Planck Institute for the Physics of Complex Systems,

Nöthnitzer Strasse 38, 01187 Dresden, Germany

(Dated: May 23, 2019)

Abstract

Single ionization of N₂, O₂ and F₂ by intense laser fields is simulated using a time-dependent density functional approach within the exchange-only local density approximation. In particular, the response to laser pulses having a wavelength of $\lambda = 390\text{nm}$ (corresponding to a frequency-doubled Ti:Sapphire laser) is investigated. Single ionization yields of N₂ and F₂ are seen to agree to within a factor of 3, in keeping with experimental results but in disagreement with predictions based on the symmetry of the highest occupied molecular orbital. The underlying mechanism for this appears to be the importance of multi-electron molecular effects in the single ionization of F₂. In addition single ionization of O₂ is calculated assuming the ground state configuration to be either a singlet or triplet state. It is discovered that the single ionization process is largely insensitive to the multiplicity of the initial state.

* Current Address: Max Planck Institute for Nuclear Physics, Saupfercheckweg 1, 69117 Heidelberg, Germany

I. INTRODUCTION

In the last two decades the interaction of atoms and molecules with intense laser pulses has attracted widespread research. This highly non-perturbative interaction results in a number of non-linear processes such as ionization, harmonic generation and above-threshold ionization. At the heart of all these processes is single electron ionization which gives rise, either directly or indirectly, to the other processes.

Compared to atoms, molecules represent a more complex class of system due to their multi-centre nature which introduces additional vibrational and rotational degrees of freedom. It is perhaps surprising therefore that the ionization of molecules by intense laser pulses share many of the characteristics with the ionization of atoms. The mechanisms of ionization can be characterized as either multiphoton transitions or tunnelling ionization, or some combination of both. The process can be classified into either the tunnelling or multiphoton regime by the Keldysh parameter, defined as $\gamma_k \equiv \sqrt{I_p/2U_p}$, where the internal binding energy is I_p and the external laser-driven kinetic energy is U_p . In the long-wavelength, intense field limit $\gamma_k \ll 1$ and tunnelling dominates and thus the excited states spectrum should play no rôle in the ionization process.

In a range of early experiments this was found to be the case: it was discovered that single ionization rates for molecules are roughly identical to those of noble gas atoms provided the ionization potentials were comparable [1, 2, 3, 4]. In one of these experiments [4] the single ionization rates of O_2 ($I_p = 12.07\text{eV}$) and of its companion noble gas atom xenon ($I_p = 12.13\text{eV}$) were measured simultaneously by exposing a target containing a mixture of xenon atoms and O_2 to a laser pulse of wavelength $\lambda = 10.6\mu\text{m}$. The ionization rates were found to be similar.

However, in later experiments carried out at Ti:Sapphire laser wavelengths ($\lambda \sim 800\text{nm}$) it was found that while most atom-molecules pairs obeyed this finding – such as N_2 ($I_p = 15.58\text{eV}$) and its companion atom argon ($I_p = 15.76\text{eV}$) – a number did not. For example, the single ionization rate of O_2 was suppressed with respect to ionization rate of xenon by several orders of magnitude [5, 6] while ionization of D_2 was also suppressed with respect to its companion noble gas atom, argon.

Considerable interest has been generated by these findings and a number of explanations have been put forward for the origin of the suppression, most notably in O_2 . Talebpour et al [5] suggested a dissociative recombination process leading to a decrease in the single ionization signal. However, later experiments [6] concluded that dissociative recombination cannot be the cause of suppression since the suppression was observed for a range of laser polarization ellipticities. An

electronic correction to tunnelling theory was suggested by Guo [7] and reproduced the correct suppression of O_2 , provided that correct parameters for an effective nuclear charge and ionization potential are chosen.

Muth-Böhm et al [8] explained the suppression of the O_2 single ionization rate using a generalization of intense-field many-body S -matrix theory (IMST) which included an interference term. They showed with their calculations that the suppression of the O_2 signal with respect to xenon, and its absence in N_2/Ar , is due to a symmetry induced dynamical effect whereby interference between ionizing wavepackets emitted from the two distinct nuclear centres is either destructive or constructive in the low energy limit, depending upon the symmetry of the highest occupied molecular orbital (HOMO). Thus for O_2 , in which the HOMO has an anti-bonding character (ground state configuration $1\sigma_g^2 1\sigma_u^2 2\sigma_g^2 2\sigma_u^2 3\sigma_g^2 1\pi_u^4 1\pi_g^2$), single ionization should show suppression. For N_2 , in which the HOMO has a bonding character (ground state configuration $1\sigma_g^2 1\sigma_u^2 2\sigma_g^2 2\sigma_u^2 3\sigma_g^2 1\pi_u^4 3\sigma_g^2$), single ionization should not be suppressed. In addition, according to the symmetry argument of IMST, when suppression does occur we can write

$$\mathbf{k}_N \cdot \mathbf{R} \ll 1, \quad (1)$$

where $k_N^2/2 = N\omega - U_p - I_p$ is the kinetic energy of the electron on absorbing N photons, ω the laser frequency and R the bond length of the molecule. Thus, if only the wavelength is varied, the suppression should be enhanced at shorter wavelengths. This explanation is consistent with the O_2/Xe results where suppression of O_2 was observed at $\lambda = 800\text{nm}$ but not at $\lambda = 10.6\mu\text{m}$.

Following the symmetry argument it was postulated that since F_2 ($I_p = 15.69\text{eV}$) has an ionization potential similar to N_2 and argon but has valence electrons with the same symmetry as O_2 (ground state configuration of F_2 : $1\sigma_g^2 1\sigma_u^2 2\sigma_g^2 2\sigma_u^2 3\sigma_g^2 1\pi_u^4 1\pi_g^4$) ionization of F_2 should also be suppressed with respect to either N_2 or argon [8]. However a later experimental study [9] showed that the ionization of F_2 is not suppressed with respect to that of N_2 .

In this paper we study the response in time of N_2 , O_2 and F_2 to laser pulses having a wavelength of 390nm and 300nm . We find single ionization suppression in O_2 and its absence in F_2 , in accordance with the experimental results at $\lambda = 800\text{nm}$. Within our framework of a time-dependent density functional approach we are able to explain the deviations from the predictions based on the symmetry of the HOMO. The paper is arranged as follows. In section II the time-dependent density functional approach is set out and the procedure for calculating single ionization rates described. In section III the time-evolution will be considered. Finally, some conclusions will be

drawn in section IV.

II. METHOD

The time-dependent density functional method provides the most detailed, practical and feasible ab initio approach for tackling many-body problems. Density functional theory (DFT), as first introduced by Hohenberg and Kohn [10] and Kohn and Sham [11] describes a system of interacting particles in terms of its density. The theory is based on the existence of an exact mapping between densities and external potentials and leads to the density of the interacting system being obtained from the density of an auxiliary system of non-interacting particles moving in an effective local single particle potential, i.e. the particle interactions are treated in an averaged-over manner. A time-dependent formalism of DFT (TDDFT) was provided by Runge and Gross [12], who showed that the time-dependent density could be obtained from the response of non-interacting particles to the time-dependent local effective potential. In principle, many-body effects are included exactly through an exchange-correlation functional; in practice, the form of this functional is unknown and at best it can only be approximated.

Such an approach has been widely used in treating the interaction of molecules with intense, short-duration laser pulses. For instance, in the approach of Chu and co-workers [13, 14] a pseudo-spectral mesh technique is used in the solution of the Kohn-Sham equations. A non-adiabatic quantum molecular dynamics (NA-QMD) method, in which the electron dynamics are treated quantum mechanically using TDDFT, has been developed by Schmidt and co-workers [16]. In this work the electron orbitals are expanded in terms of Gaussian basis functions. More recently, Castro et al [17] developed grid-based NA-QMD technique to study harmonic generation in H_2 . However, these calculations were limited to a 1D treatment of the electron dynamics. Another grid-based DFT method has been developed by Otobe et al [15]. While this method has calculated tunnel ionization rates for N_2 , O_2 and F_2 two approximations have been made. Firstly, a pseudo-potential description of the electron-nuclear potential was used meaning that only the valence electrons in the molecules were treated. Secondly, only static field ionization rates were calculated.

The current approach utilizes a NA-QMD approach in which the electron dynamics are described by a hybrid finite difference-Lagrange mesh technique [18]. For the present calculations, however, a fixed nuclei description has been employed. Details of the approach are now given.

A. Time-dependent Kohn-Sham equations

In the TDDFT approach, the total N_e -electron Kohn-Sham wavefunction is written as a single determinant of one-particle Kohn-Sham orbitals. Denoting the spin state of each orbital by the label $\sigma = \uparrow, \downarrow$, we can write the electron density as

$$n(\mathbf{r}, t) = \sum_{\sigma=\uparrow, \downarrow} n_{\sigma}(\mathbf{r}, t) = \sum_{\sigma=\uparrow, \downarrow} \sum_{i=1}^{N_{\sigma}} |\psi_{i\sigma}(\mathbf{r}, t)|^2, \quad (2)$$

where N_{σ} is the number of electrons in spin state σ and $\psi_{i\sigma}(\mathbf{r}, t)$ are the Kohn-Sham orbitals. The orbitals are obtained through the solution of the time-dependent Kohn-Sham equations

$$i \frac{\partial}{\partial t} \psi_{i\sigma}(\mathbf{r}, t) = \left[-\frac{1}{2} \nabla^2 + V_{\text{eff}}(\mathbf{r}, t) \right] \psi_{i\sigma}(\mathbf{r}, t), \quad (3)$$

where

$$V_{\text{eff}}(\mathbf{r}, t) = V_{\text{ext}}(\mathbf{r}, \mathbf{R}, t) + V_H(\mathbf{r}, t) + V_{xc\sigma}(\mathbf{r}, t), \quad (4)$$

is the time-dependent effective potential which is given in terms of the external potential

$$V_{\text{ext}}(\mathbf{r}_i, \mathbf{R}, t) = V_{\text{ions}}(\mathbf{r}_i, \mathbf{R}, t) + U_{\text{elec}}(\mathbf{r}_i, t), \quad (5)$$

where $U_{\text{elec}}(\mathbf{r}_i, t)$ denotes the interaction between electron i and the applied laser field and where

$$V_{\text{ions}}(\mathbf{r}_i, \mathbf{R}, t) = \sum_{I=1}^{N_n} V_{\text{ion}}(\mathbf{r}_i, \mathbf{R}_I, t) = - \sum_{I=1}^{N_n} \frac{Z_I}{|\mathbf{R}_I - \mathbf{r}_i|}, \quad (6)$$

denotes the Coulomb interaction between electron i and all ions. The time-dependent effective potential also depends on the Hartree potential

$$V_H(\mathbf{r}, t) = \int d\mathbf{r}' \frac{n(\mathbf{r}', t)}{|\mathbf{r} - \mathbf{r}'|}, \quad (7)$$

and the exchange-correlation potential

$$V_{xc\sigma}(\mathbf{r}, t) = \frac{\delta E_{xc}[n_{\uparrow}, n_{\downarrow}]}{\delta n_{\sigma}} \bigg|_{n_{\sigma}=n_{\sigma}(\mathbf{r}, t)}, \quad (8)$$

where $E_{xc}[n_{\uparrow}, n_{\downarrow}]$ is the exchange-correlation action.

B. Treatment of the exchange-correlation potential

All many-body effects are included within the exchange-correlation potential, which in practice must be approximated. While many sophisticated approximations to this potential have been developed [19], the simplest is the adiabatic local density approximation in the exchange-only limit

(xLDA). In this case the exchange energy functional is given by

$$E_x[n_\uparrow, n_\downarrow] = -\frac{3}{2} \left(\frac{3}{4\pi} \right)^{1/3} \sum_{\sigma=\uparrow,\downarrow} \int d\mathbf{r} n_\sigma^{4/3}(\mathbf{r}, t), \quad (9)$$

from which the exchange-correlation potential

$$V_{xc\sigma}(\mathbf{r}, t) = - \left(\frac{6}{\pi} \right)^{1/3} n_\sigma^{1/3}(\mathbf{r}, t), \quad (10)$$

can be obtained. This approximate functional is easy to implement and is one of the most widely used exchange-correlation functionals. However, it does suffer from a number of drawbacks, most notably it contains self-interaction errors. This self-interaction means that the asymptotic form of the potential is exponential instead of Coulombic. Therefore, the electronic properties and response of the system can differ markedly from those of the actual system (as we shall see, for example in section III A).

C. Numerical details

Precise numerical details of how the code is implemented are given in [18]. Briefly, the numerical implementation of TDDFT uses a cylindrical grid treatment of the electronic Kohn-Sham orbitals. As in [22] a finite difference treatment of the z -coordinate and a Lagrange mesh treatment of the ρ -coordinate based upon Laguerre polynomials is used. For the case of diatomic molecules and considering a linearly polarized laser pulse with the laser polarization direction parallel to the molecular axis the azimuthal angle ϕ can be treated analytically. The time-dependent Kohn-Sham equations of TDDFT are discretized in space using these grid techniques and the resulting computer code parallelized to run on massively-parallel processors. Several parameters in the code affect the accuracy of the method. These are the number of points in the finite difference grid (N_z), the finite difference grid spacing (Δz), the number of Lagrange-Laguerre mesh points (N_ρ), the scaling parameter of the Lagrange-Laguerre mesh (h_ρ), the order of the time propagator (N_t) and the time spacing (Δt) [18]. In all the calculations presented here, converged results were obtained using the following parameters (atomic units are used throughout): $N_z = 2291$, $\Delta z = 0.05$, $N_\rho = 43$, $h_\rho = 0.28838771$, $N_t = 18$ and $\Delta t = 0.02$. The code was parallelized and the calculations were carried out using 79 processors.

D. Determination of Ionization

Within TDDFT all observables are functionals of the electronic density. However, as in the case of the exchange correlation functional, the exact forms of these functionals may not be known and must therefore be approximated. The functional describing ionization falls into this category. To date, most calculations of ionization within TDDFT have been obtained using geometric properties of the time-dependent Kohn-Sham orbitals [20]. Briefly, an analysing box is introduced as a way to approximately separate the bound- and continuum-state parts of the wavefunction. We define the box such that all relevant bound states of the wavefunction are contained inside this box while the continuum contributions are found outside the box. In that case the number of bound electrons is given by

$$N_{\text{bound}}(t) = \int_{\text{inside box}} d\mathbf{r} n(\mathbf{r}, t), \quad (11)$$

while the number of continuum electrons is given by

$$N_{\text{esc}}(t) = \int_{\text{outside box}} d\mathbf{r} n(\mathbf{r}, t). \quad (12)$$

We then define the number of bound and continuum electrons for each Kohn-Sham orbital as (dropping spin subscripts)

$$N_j(t) = \int_{\text{inside box}} d\mathbf{r} |\psi_j(\mathbf{r}, t)|^2, \quad (13)$$

for bound electrons and

$$\overline{N}_j(t) = \int_{\text{outside box}} d\mathbf{r} |\psi_j(\mathbf{r}, t)|^2, \quad (14)$$

for continuum electrons. Thus we obtain approximate ion probabilities, $P^k(t)$, for charge state k . In particular we find

$$P^0(t) = N_1(t) \cdots N_{N_e}(t), \quad (15)$$

and

$$P^1(t) = \sum_{n=1}^{N_e} N_1(t) \cdots \overline{N}_n(t) \cdots N_{N_e}(t). \quad (16)$$

III. RESULTS

We now study the response of N_2 , O_2 and F_2 to intense laser pulses. Firstly, we compute the ionization potentials of the various molecules. Then we compare single ionization of N_2 and F_2 showing that the F_2^+ yield shows no suppression with respect to the N_2^+ yield. Thirdly, we

compare the yields of O_2^+ using two initial configurations of the molecule, namely a singlet and a triplet state. This shows that the suppression of the O_2^+ signal is not due to the fact that the O_2 ground state is a triplet configuration. In order to gain a better understanding of the electronic dynamics we analyse the time-evolution of the Kohn-Sham orbitals, showing that in the case of F_2 the response of the core electrons show a significant response to the pulse.

A. Ionization Potentials

The starting point for any simulation of the response of diatomic molecules to intense laser pulses is an appropriate description of the field-free structure. In our calculations we assume that the molecules are initially in their ground states. Starting from the equilibrium ion separation the ground state electronic density is calculated self-consistently from the time-dependent Kohn-Sham equations using an iterative Lanczos method [21, 22]. Of particular importance in the present calculations are the ionization potentials of the different molecules. These are obtained by first calculating the ground state energy of the particular molecule and then that of the molecule with one electron removed. The results are presented in table I for N_2 , O_2 and F_2 . We see that the ionization potentials of N_2 and O_2 compare well to the experimental values [23] while the ionization potential of F_2 shows a 10% difference with the experimental value. The difference can be explained in terms of the choice of exchange-correlation potential, as discussed earlier. Obviously in comparing single ionization in N_2 and F_2 the errors in their ionization potentials will have an important impact upon their subsequent response. It has been pointed out to us [24] that the 10% decrease in the ionization potential of F_2 could increase the single ionization yield by two orders of magnitude. However, such an estimation, obtained using IMST, only takes into account the response of the HOMO to the field. As our results will show, it appears that molecular effects due to the other orbitals are extremely important in this system and such a large increase in ionization yield due to a lowering of the ionization potential is unlikely. This is supported by the static field tunnel ionization calculations of Otobe et al [15] who employed a DFT approach using the self-interaction free KLI approximation. In these calculation the ionization potential of F_2 was much closer to the experimental value. However, no suppression of the F_2^+ signal was evident.

B. Single ionization yields of N_2 and F_2

Table II presents a comparison of the single ionization yields for N_2^+ and F_2^+ after the interaction of the neutral molecules with a 24 cycle laser pulse (pulse length, $\tau = 31.2\text{fs}$) having a wavelength of $\lambda = 390\text{nm}$ over the intensity range $I = 1 \times 10^{14} \text{ W/cm}^2$ to $I = 8 \times 10^{14} \text{ W/cm}^2$. As discussed in the introduction, if the symmetry induced dynamical effect is responsible for ionization suppression, equation (1) predicts that the yield of F_2^+ ions should be suppressed to a greater extent to the yield of N_2^+ ions at the wavelength used in these calculations. While differences do exist between the N_2^+ and F_2^+ ion yields, we see that the differences are no more than a factor of three. We conclude that *single ionization of F_2 is not suppressed with respect to the single ionization of N_2 .*

C. Single ionization yields from $^1\text{O}_2$ and $^3\text{O}_2$

One explanation postulated for the nonatomiclike single ionization in O_2 compared to single ionization of N_2 is the fact that the ground state of O_2 is a triplet state with a half-filled open-shell structure whereas the ground state of N_2 is a singlet state with a closed-shell structure [6]. Müth-Bohm et al [8] argued that such a difference in the spin states is unlikely to influence the ionization signal since the spin-degrees of freedom are not effectively coupled to a dipole field. We are unaware of any calculation to date in which single ionization of O_2 is studied as a function of the multiplicity of the ground state.

Table III compares the single ionization yields of $^1\text{O}_2$ and $^3\text{O}_2$ at the end of a 24 cycle laser pulse ($\tau = 31.2\text{fs}$) having a wavelength of $\lambda = 390\text{nm}$ over the intensity range $I = 1 \times 10^{14} \text{ W/cm}^2$ to $I = 8 \times 10^{14} \text{ W/cm}^2$. We see that no significant difference of the yields due to the two configurations is evident. Hence, we conclude that *the suppression of O_2^+ with respect to that of Xe^+ is not due to the ground state of O_2 being a triplet state.*

D. Orbital response of N_2 , O_2 and F_2

In order to gain a better understanding of the ionization dynamics we have investigated the time evolution of the Kohn-Sham orbitals. It must be stressed that these orbitals do not have any physical significance with the molecular orbitals of the actual system. However, studying the evolution of the Kohn-Sham orbitals allows us to obtain information about the orbital symmetries. In

figure 1 we present results for the time-evolution of the Kohn-Sham orbitals of N_2 during its interaction with a 24 cycle laser pulse of wavelength $\lambda = 390\text{nm}$. Two laser intensities are presented: $I = 1 \times 10^{14} \text{ W/cm}^2$ and $I = 6 \times 10^{14} \text{ W/cm}^2$. It can clearly be seen that the orbital having the same symmetry ($3\sigma_g$) as the valence orbital of N_2 shows the dominant response to the field. The same behaviour is observed for all other laser intensities considered in table II. Thus it is apparent that single ionization of N_2 occurs predominantly by ionization of the valence electron. Since the valence orbital of N_2 has a bonding character then, based upon the symmetry arguments of IMST, we would expect no ionization suppression to occur – as is the case.

In figure 2 we present results for the time-evolution of the Kohn-Sham orbitals of O_2 during its interaction with a 24 cycle laser pulse of wavelength $\lambda = 390\text{nm}$. Again, two laser intensities are presented: $I = 1 \times 10^{14} \text{ W/cm}^2$ and $I = 6 \times 10^{14} \text{ W/cm}^2$. As in the case of N_2 we see that the orbital having the same symmetry ($1\pi_g$) as the valence orbital of O_2 shows the dominant response to the field and thus single ionization of O_2 occurs predominantly by ionization of the valence electron. Since the valence orbital of O_2 has an anti-bonding character then, based upon the symmetry argument of IMST, we would expect ionization suppression to occur – again, in accordance with the numerical results and experiment.

In figure 3 we present results for the time-evolution of the Kohn-Sham orbitals of F_2 during its interaction with a 24 cycle laser pulse of wavelength $\lambda = 390\text{nm}$. Four laser intensities are presented: $I = 1 \times 10^{14} \text{ W/cm}^2$, $I = 2 \times 10^{14} \text{ W/cm}^2$, $I = 4 \times 10^{14} \text{ W/cm}^2$ and $I = 6 \times 10^{14} \text{ W/cm}^2$. It is apparent that the orbital having the same symmetry ($1\pi_g$) as the valence orbital of F_2 does not in this case show the dominant response to the field. Instead we see that for all of the intensities, apart from $I = 1 \times 10^{14} \text{ W/cm}^2$, the orbital having the symmetry $3\sigma_g$ shows the dominant response. Since this orbital has a bonding character then, based upon the predictions of IMST, ionization suppression will not occur. We conclude that single ionization of F_2 does not occur predominantly by ionization of the valence electron. Thus, molecular structure effects for this molecule are of crucial importance.

In understanding why the orbital having the same symmetry ($1\pi_g$) as the valence orbital of F_2 does not respond predominantly to the field we consider the response of F_2 at the laser intensity of $I = 1 \times 10^{14} \text{ W/cm}^2$ where the $3\sigma_g$ orbital did not show the dominant response to the field. In this case the $1\pi_g$ anti-bonding orbital and the $1\pi_u$ bonding orbital showed the dominant response. Indeed we see that over all laser intensities these two orbitals response in a similar fashion to the field. It would therefore appear that an interference is occurring between these two orbitals.

To gain further insight we have repeated the TDDFT calculations at the laser intensity of $I = 2 \times 10^{14} \text{ W/cm}^2$, whereby only a subset of the orbitals were allowed to respond to the field, all other orbitals being frozen. The results are presented in figure 4. We see from figure 4(c) that when only the $1\pi_u$ and $1\pi_g$ orbitals respond to the field, ionization is suppressed. In figures 4(a) and 4(b) we see that the ionization of either the $1\pi_u$ or $1\pi_g$ is greater than that of the $3\sigma_g$ orbital. In figure 4(d), when the $3\sigma_g$, $1\pi_u$ and $1\pi_g$ orbitals respond, ionization of the $3\sigma_g$ is dominant. This behavior illustrates a rather complicated correlated response of the orbitals to the laser field. Moreover, from figure 3 we can see that a resonance effect is coming into play. This is evidenced at the laser intensities of $I = 4 \times 10^{14} \text{ W/cm}^2$ and $I = 6 \times 10^{14} \text{ W/cm}^2$ where the rate of depletion of the $1\pi_u$ and $1\pi_g$ orbitals is not exponential but instead shows evidence of two distinct rates being present, namely an intermediate resonance state is initially populated and then undergoes ionization itself. Figure 5 presents results for the time-evolution of the Kohn-Sham orbitals of F_2 during its interaction with a 24 cycle laser pulse of wavelength $\lambda = 300\text{nm}$ at laser intensities $I = 4 \times 10^{14} \text{ W/cm}^2$ and $I = 6 \times 10^{14} \text{ W/cm}^2$. In this case the orbital populations are depleted exponentially, thus confirming the presence of the resonance at $\lambda = 390\text{nm}$.

Hence, we confirm the connection of the suppression of ionization with destructive interference of outgoing electron waves from the ionized electron orbital as put forward first by Muth-Böhm et al. [8]. However, the prediction of ionization suppression justified within the IMST approach through the symmetry of the HOMO is not reliable, since it turns out that, e.g., in the case of F_2 the electronic response to the laser pulse is rather complicated and does not lead to dominant depletion of the HOMO. Therefore, the symmetry of the HOMO is not sufficient to predict ionization suppression. However, at least for F_2 , the symmetry of the dominantly ionized orbital is consistent with the non-suppression of ionization.

IV. SUMMARY

Single ionization of N_2 , O_2 and F_2 by intense laser fields having a wavelength of $\lambda = 390\text{nm}$ has been simulated using a time-dependent density functional approach within the exchange-only local density approximation. The results obtained for the single ionization of N_2 and O_2 are in agreement with IMST results [8], if the HOMO is dominantly ionized. This is the case for N_2 and O_2 , where for the latter molecule destructive interference leads to a suppression of ionization. In addition it is found that the suppressed ionization of O_2 with respect to its companion noble gas

atom (xenon) does not arise from the multiplicity of the ground state of O_2 .

For single ionization of F_2 , it is found that the ionization signal is not suppressed with respect to the N_2^+ yield, in keeping with other static-field TDDFT results [15]. Multielectron molecular correlation leads to the dominant ionization of an orbital with symmetry different from the one of the HOMO. This is the reason why the prediction based on the symmetry of the HOMO fails [8].

The present calculations are carried out within xLDA. Implementations of TDDFT which go beyond the xLDA approximation to a self-interaction free exchange-correlation potential improve the description of the ionization potentials and will be the focus of future work. In addition only parallel transition have been considered in this paper which is a reasonable approximation for strong field ionization of diatomics. Future work will focus on generalizing the calculations of single ionization rates to arbitrary orientations between the molecular axis and the laser polarization direction.

Acknowledgments

The authors would like to acknowledge useful discussions with Andreas Becker. The work reported in this paper is supported by the UK Engineering and Physical Sciences Research Council by provision computer resources at Computer Services for Academic Research, University of Manchester and HPC(X), Daresbury Laboratory.

- [1] G.N. Gibson, R.R. Freeman and T.J. McIlrath, *Phys. Rev. Lett.* **67**, 1230 (1991)
- [2] S.L. Chin, Y. Liang, J.E. Decker, F.A. Ilkov and M.V. Ammosov, *J. Phys. B: At. Mol. Opt. Phys.* **25**, L249 (1992)
- [3] T.D.G Walsh, J.E. Decker and S.L. Chin, *J. Phys. B: At. Mol. Opt. Phys.* **26**, L85 (1993)
- [4] T.D.G. Walsh, F.A. Ilkov, J.E. Decker, and S.L. Chin, *J. Phys. B: At. Mol. Opt. Phys.* **27**, 3767 (1994)
- [5] A. Talebpour, C.-Y. Chien and S.L. Chin, *J. Phys. B: At. Mol. Opt. Phys.* **29**, L677 (1996)
- [6] C. Guo, M. Li, J.P. Nibarger and G.N. Gibson, *Phys. Rev. A* **58**, R4271 (1998)
- [7] Guo C, *Phys. Rev. Lett.* **85**, 2276 (2000)
- [8] J. Muth-Böhm, A. Becker and F.H.M. Faisal, *Phys. Rev. Lett.* **85**, 2280 (2000)
- [9] M.J. DeWitt, E. Wells and R.R. Jones, *Phys. Rev. Lett.* **87**, 153001 (2001)
- [10] P. Hohenberg and W. Kohn, *Phys. Rev.* **136**, B864 (1964)

- [11] W. Kohn and L.J. Sham, Phys. Rev. **140**, A1133 (1965)
- [12] E. Runge and E.K.U. Gross, Phys. Rev. Lett. **52**, 997 (1984)
- [13] X. Chu & S.-I. Chu, Phys. Rev. A **63**, 023441 (2001)
- [14] X. Chu & S.-I. Chu, Phys. Rev. A **64**, 063404 (2001)
- [15] T. Otobe, K. Yabana and J.-I. Iwata, Phys. Rev. A **69**, 053404 (2004)
- [16] M. Uhlmann, T. Kunert, F. Grossmann and R. Schmidt, Phys. Rev. A **67**, 013413 (2003)
- [17] A. Castro, M.A.L. Marques, J.A. Alonso, G.F. Bertsch and A. Rubio, Eur. Phys. J. D **28**, 211 (2004)
- [18] D. Dundas, J. Phys. B: At. Mol. Opt. Phys. **37**, 2883 (2004)
- [19] J. Kohanoff and Gidopoulos *Handbook of Molecular Physics and Quantum Chemistry* ed Wilson S (John Wiley and Sons Ltd, Chichester, 2003)
- [20] C.A. Ullrich, J. Mol. Struc. - Theochem **501**, 315 (2000)
- [21] E.S. Smyth, J.S. Parker and K.T. Taylor, Comp Phys Commun **114**, 1 (1998)
- [22] D. Dundas, Phys. Rev. A **65**, 023408 (2002)
- [23] K.P. Huber and G. Herzberg, *Constants of Diatomic Molecules*, in NIST Chemistry WebBook Vol. 69, edited by P.J. Lindstrom and W.G. Mallard (National Institute of Standards and Technology, Gaithersburg, 2003).
- [24] A. Becker, private communication.

Ionization Potential (eV)			
	N ₂	O ₂	F ₂
Present	15.91	11.45	14.14
Exact	15.58	12.07	15.69

TABLE I: Ionization potentials of N₂, O₂ and F₂ calculated using a TDDFT approach within the exchange-only local density approximation compared with the experimental values [23]. While the ionization potentials of N₂ and O₂ agree to within 5%, those for F₂ differ by 10%.

Laser Intensity ($\times 10^{14}$ W/cm ²)	Ion Yields	
	N ₂ ⁺	F ₂ ⁺
1.0	0.2479176	0.1051454
2.0	0.3804471	0.2523075
4.0	0.4025715	0.3742050
6.0	0.3501940	0.3278126
8.0	0.2919808	0.3375370

TABLE II: Ion yields of N₂⁺ and F₂⁺ after interaction of the neutral molecules with a 24 cycle laser pulse having a wavelength of $\lambda = 390$ nm for a range of laser intensities. The ion yields differ by factor of less than 3. Hence, the F₂⁺ yield is not suppressed with respect to the N₂⁺ yield.

Laser Intensity ($\times 10^{14}$ W/cm 2)	Ion Yield	
	$^1\text{O}_2 \rightarrow \text{O}_2^+$	$^3\text{O}_2 \rightarrow \text{O}_2^+$
1.0	0.0009385	0.0006335
2.0	0.0022583	0.0017794
4.0	0.0038756	0.0032043
6.0	0.0041731	0.0033902
8.0	0.0036198	0.0027161

TABLE III: Ion yields of O_2^+ (assuming either an initial singlet or triplet configuration of the neutral O_2 molecule) after interaction with a 24 cycle laser pulse having a wavelength of $\lambda = 390\text{nm}$ for a range of laser intensities. The ion yields roughly agree, indicating that the multiplicity of the ground state of O_2 do not play a rôle in the suppression of the O_2^+ yield.

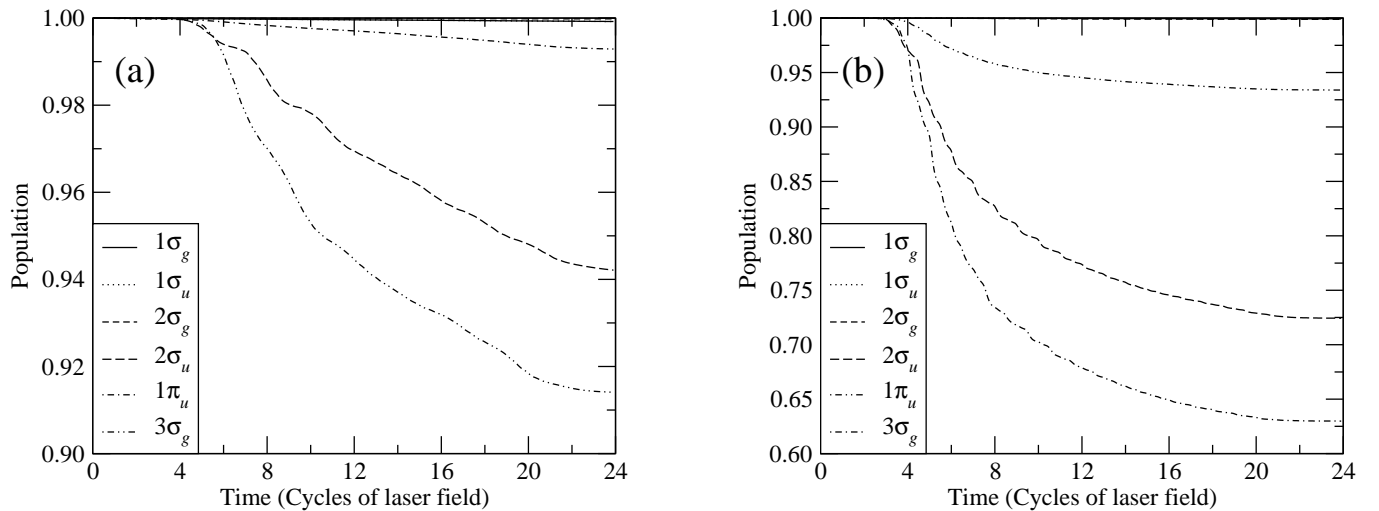


FIG. 1: Kohn-Sham orbital populations for N_2 during interaction with a 24 cycle laser pulse having a wavelength of $\lambda = 390\text{nm}$ and laser intensity (a) $I = 1 \times 10^{14} \text{ W/cm}^2$ and (b) $I = 6 \times 10^{14} \text{ W/cm}^2$. For all laser intensities it is seen that the Kohn-Sham orbital having the same symmetry ($3\sigma_g$) as the valence orbital of N_2 shows the predominant response to the field.

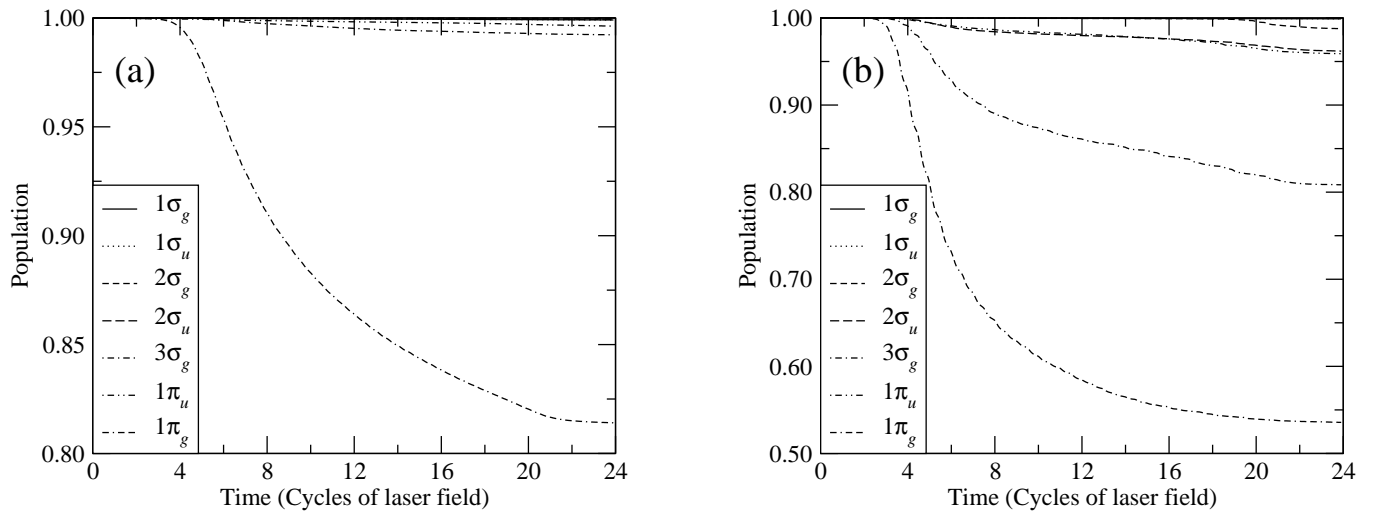


FIG. 2: Kohn-Sham orbital populations for O_2 during interaction with a 24 cycle laser pulse having a wavelength of $\lambda = 390\text{nm}$ and laser intensity (a) $I = 1 \times 10^{14} \text{ W/cm}^2$ and (b) $I = 6 \times 10^{14} \text{ W/cm}^2$. For all laser intensities it is seen that the Kohn-Sham orbital having the same symmetry ($1\pi_g$) as the valence orbital of O_2 shows the predominant response to the field.

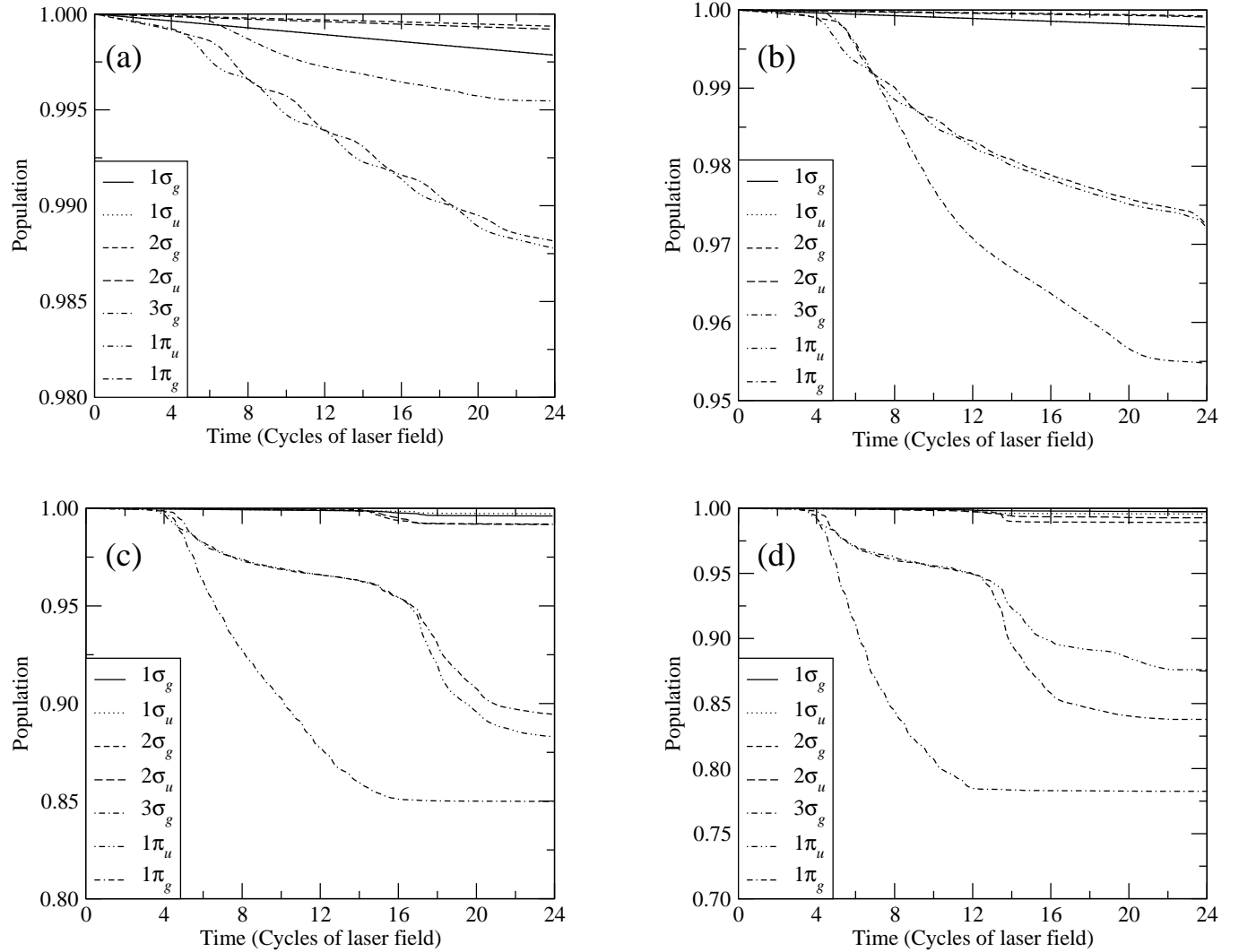


FIG. 3: Kohn-Sham orbital populations for F_2 during interaction with a 24 cycle laser pulse having a wavelength of $\lambda = 390\text{nm}$ and laser intensity (a) $I = 1 \times 10^{14} \text{ W/cm}^2$, (b) $I = 2 \times 10^{14} \text{ W/cm}^2$, (c) $I = 4 \times 10^{14} \text{ W/cm}^2$ and (d) $I = 6 \times 10^{14} \text{ W/cm}^2$. For all laser intensities, except $I = 1 \times 10^{14} \text{ W/cm}^2$, it is seen that the $3\sigma_g$ orbital predominantly responds to the field. At the lowest intensity the $1\pi_g$ anti-bonding orbital (having the same symmetry as the valence orbital of F_2) is equally dominant with the $1\pi_u$ bonding orbital. These two orbitals respond almost identically at all laser intensities.

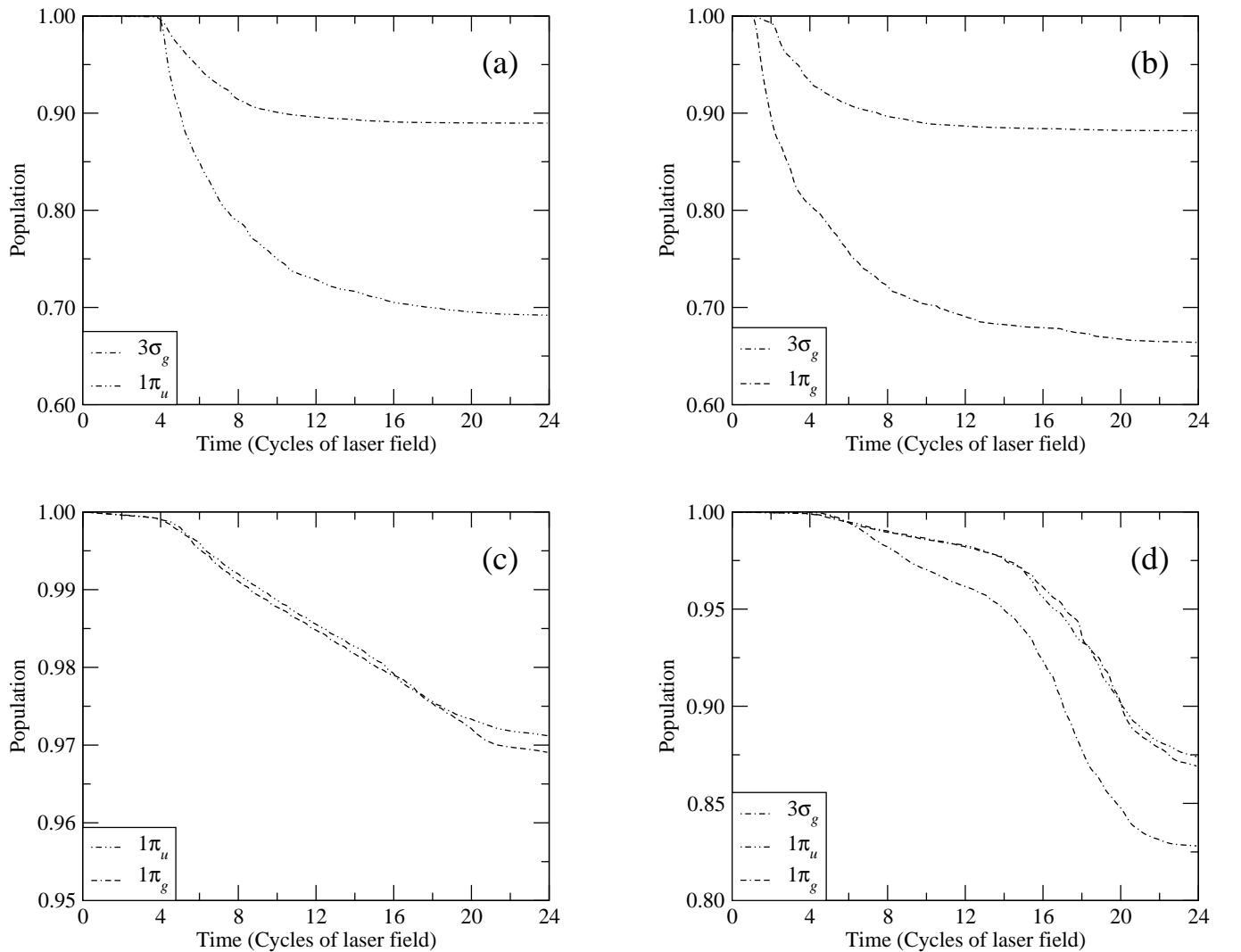


FIG. 4: Kohn-Sham orbital populations for F_2 during interaction with a 24 cycle laser pulse having a wavelength of $\lambda = 390\text{nm}$ and an intensity of $I = 2 \times 10^{14} \text{ W/cm}^2$. In these calculations only the orbitals shown in each figure respond to the field. All other orbitals are frozen. It can clearly be seen in (c) that when only the $1\pi_u$ and $1\pi_g$ orbitals respond to the field, ionization is suppressed. In (a) and (b) we see that the ionization of either the $1\pi_u$ or $1\pi_g$ is greater than that of the $3\sigma_g$ orbital. When the $3\sigma_g$, $1\pi_u$ and $1\pi_g$ orbitals respond, however, ionization of the $3\sigma_g$ orbital is dominant.

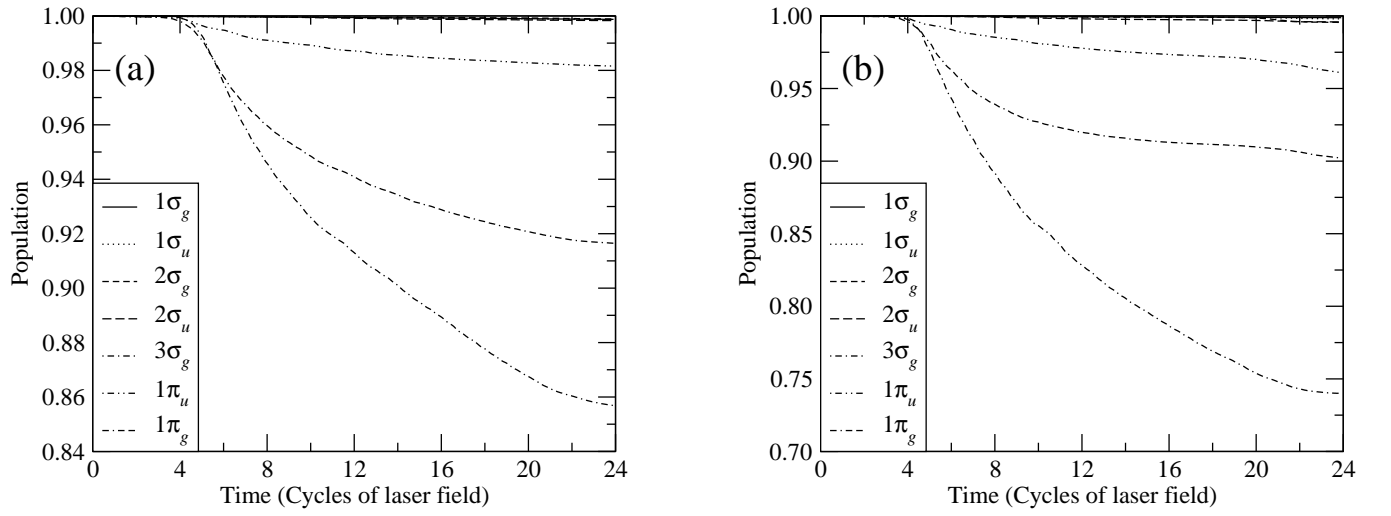


FIG. 5: Kohn-Sham orbital populations for F_2 during interaction with a 24 cycle laser pulse having a wavelength of $\lambda = 300\text{nm}$ and intensity (a) $I = 4 \times 10^{14} \text{ W/cm}^2$ and (b) $I = 6 \times 10^{14} \text{ W/cm}^2$. At this laser wavelength we see that the the orbital populations fall off exponentially, unlike the response at $\lambda = 390\text{nm}$ observed in figure 3. We conclude that the response at $\lambda = 390\text{nm}$ is due to the population of an intermediate resonance state.